A Novel Filtered Backprojection-Based Algorithm for Sparse View CT Image Reconstruction

Meng Wu, Andreas Maier, Qiao Yang, and Rebecca Fahrig

***Abstract*—The limited number of projections causes view aliasing artifacts in filtered backprojection (FBP) CT reconstructions. The view artifacts appear as streak artifacts or blurring in the azimuthal direction. We propose an FBP-based algorithm using a view aliasing free reconstruction to identify the structures in projection spaces that may cause the artifacts. A feature preserving interpolation in projection space is used to increase the view sampling rate. The restored high frequency structures are then added back to the view aliasing free reconstruction. Numerical simulations show the proposed method reduces the view aliasing artifacts for downsampling rates of 4 to 8, and its mean absolute error is smaller than the linear interpolation method.**

***Index Terms*—CT, reconstruction, FBP, sparse view**

I. Introduction

The reasons for CT scans with a small number of projections are the limited detector readout rate or intentional radiation dose reduction. Using total variation constrained iterative reconstructions for view undersampled data has shown the ability to provide good image quality, but usually has long computation time [1], [2]. In addition, the iterative method often relies on the piecewise constant regularization or a prior image, which may cause additional difficulties when interpreting the images [3].

In the conventional filtered backprojection (FBP) reconstruction method, some high frequency structures that are not supported by the angular sampling rate may cause view undersampling artifacts. Several analytical methods based on interpolation in projection space have also been proposed [4]–[6]. The view interpolation can increase the number of angular samples, but the shapes and the positions of some high frequency structures may not be correct in the interpolated projections. There are more advanced interpolation methods called directional sinogram interpolation that generate more projections by optimized double-orientation estimation in sinogram space and directional interpolation [5]. The challenge of view interpolation based approaches is that the high frequency structures may hide inside the total line integral of the whole object. The interpolation methods usually match the changes of the total line integral and ignore the small structures that cause the view aliasing artifacts in the reconstruction.

In this paper, we describe a novel FBP based algorithm with only a few iterations that reduces the view aliasing artifact in the image reconstruction. Our approach starts with an FBP reconstruction without view aliasing artifacts, and gradually add reconstructions of the high frequency structures using a feature-preserving interpolation. The restored high frequency structures may have better accuracy in shape and position.

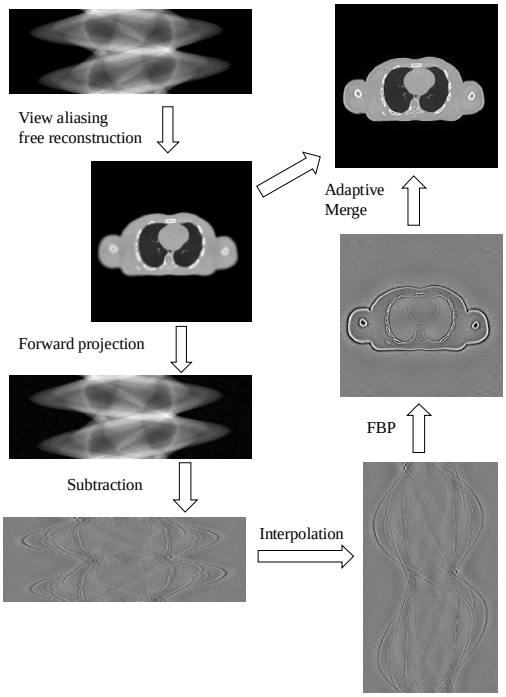

Fig. 1: Schematic workflow of proposed algorithm.

II. Methods

Only one pass of interpolation of the total line integral (sinogram) cannot accurately increase angular sampling rate of all structures or completely remove view aliasing artifacts. Moreover, the small structures that are more likely to cause artifacts are often difficult to recognize in the total line integral of the whole object. Therefore, identification and separation of those small structures may help to increase the accuracy of interpolation. The proposed algorithm has the following main steps:

1. Reconstruct images without view aliasing artifacts.
2. Extract high frequency structures in projection space.
3. Feature preserving interpolation in projection space.
4. Restore high frequency structures.

M. Wu and R. Fahrig are with the Department of Radiology, Stanford University, USA e-mail:mengwu@stanford.edu.

A. Maier and Q. Yang are with Pattern Recognition Lab, Friedrich-Alexander University of Erlangen-Nrnberg, Germany.

This work is supported by Erlangen Graduate School in Advanced Optical Technologies.

The schematic workflow of the proposed algorithm is shown in Figure 1. In the following sections, we will describe each step in details.

A. Reconstruct images without view aliasing artifacts

The first task is to reconstruction an image that does not have view aliasing artifacts. In other word, the image will have locally highest resolution that is support by the scan angular sampling rate. In the CT scan, the Nyquist angular sampling rate is not uniform over the entire axial plane. The Nyquist angular sampling rate at the center of the rotation is much lower than that at the edge of the FOV.

Assuming a parallel beam geometry, the point at distant s from the center of rotation has corresponding spatial frequency spaced by $\Delta v = \frac{1}{2s}$. For fixed scan angular sampling spacing $\Delta\beta$, the proper detector radial sampling spacing Δ_R satisfies

$$\frac{1}{2\Delta_R} \cdot \Delta\beta = \Delta v. \tag{1}$$

Thus, for this image point, the supported minimum radial samples spacing is

$$\widetilde{\Delta_R} = \frac{\Delta\beta}{2\Delta v} = s \cdot \Delta\beta. \tag{2}$$

To avoid view aliasing, the image has to be reconstructed with different radial sample spacing according to the distance from the center of rotation. This is, as we move away from the center of rotation, the image should be reconstructed at progressively lower resolution (or frequency).

The acquired detector data usually has much higher sampling rate than the maximum supported radial frequency. Thus, the high frequency components of the projection data have to be cut off before the backprojection to generate a view aliasing free reconstruction. The FBP reconstruction can be written as

$$g(\vec{x}) = \sum \frac{1}{l^2(\vec{x})} \mathcal{B}((w \cdot y(u,\beta)) * h, \beta)\Delta\beta, \tag{3}$$

where $g(\vec{x})$ denotes reconstructed image at position $\vec{x}$; $y(u,\beta)$ denotes the logged projection data at lateral position u and angle β; w denotes a cosine and short scan weighting factor; h denotes the ramp filter; $\mathcal{B}$ denotes the backprojection operator; $l(\vec{x})$ denotes the magnification factor. To adaptively change the frequency rate, we can split the ramp filter into several frequency segments, and combine the frequency segments of the filtered projections according to the position of the reconstructed point as

$$g(\vec{x}) = \sum c_i(\vec{x}) \sum \frac{1}{l^2(\vec{x})} \mathcal{B}((w \cdot y(u,\beta)) * h_i, \beta)\Delta\beta, \tag{4}$$

where h_i denotes the ith frequency segment of ramp filter with the center frequency of the segment f_i; $c_i(\vec{x})$ denotes the combining weight of the ith frequency segment of the filtered projection for image position $\vec{x}$. To have a smooth transition, we calculated the combining weights using

$$c_i(\vec{x}) = \frac{1}{1 + \exp(10(f_i \cdot \widetilde{\Delta_R} - 1))}, \tag{5}$$

where $\widetilde{\Delta_R}$ is calculated by Eqn. (2) using $\vec{x}$. In this work, we split the ramp filter using eight triangle functions. Figure 2 shows frequency split of the ramp filter and resulting filter at the different reconstruction positions. Figure 3 shows an example of view aliasing free reconstruction. The resolution at center is much higher than the resolution at the boundary. Note that, there are no streak artifacts because there is no view aliasing.

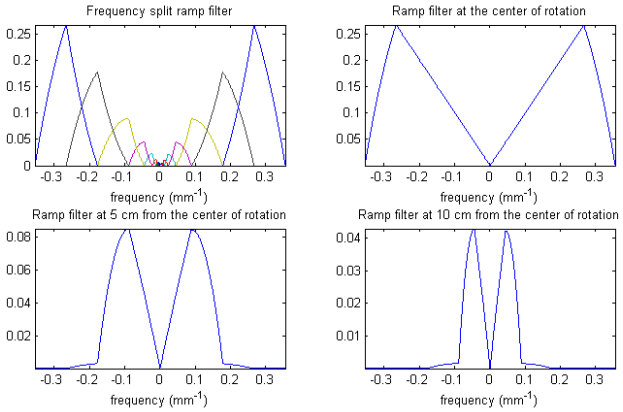

Fig. 2: Frequency split of the ramp filter and resulting filters at the different reconstruction positions.

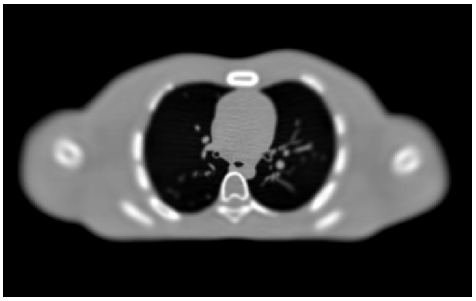

Fig. 3: An example of view aliasing free reconstruction with view downsampling rate 8. Display window [-750 750] HU.

B. Extract aliasing structures in the projection space

The view aliasing free image provides the knowledge of the structures that are supported by the current angular sampling rate. The view aliasing free image can also be used to extract the high frequency structures that may cause view aliasing artifacts. Since we cannot restore those high frequency structures in the image space for given scan data, we need to extract and upsample in the projection space. To extract the projection of the high frequency structures, we simply subtract the projections of the view aliasing free image from the measured data. The remaining signals after the subtraction are the source of the view aliasing artifacts in the FBP reconstruction.

C. Feature preserving interpolation

After extracting the projections of the structures that may cause view aliasing artifacts, we can use interpolation to increase the angular sampling rate of those structures in projection space. In the interpolation, we assume the shapes

of the structures in the projections do not change significantly in adjacent views. The differences between two adjacent projections are modeled as motions of structures caused by view angle changes. Moreover, when the angular difference is small, the movement of the position of one structure on the sinogram is linear. Based on those two assumptions, we proposed a feature preserving interpolation to up-sample the sinogram. For each pair of adjacent projections, both forward and backward motion estimation is conducted with a correlation measurement as in [7]. The interpolated projections may have the more accurate shapes and positions of the high frequency structures to compensate for the streak and blurring artifacts caused by view aliasing.

The feature preserving interpolation process finds similar local structures in two adjacent projections, and replicates those structures in the interpolated projection. Mathematically, the interpolation can by expressed as

$$\tilde{y}(u, \frac{\beta_1+\beta_2}{2}) = \frac{y(u-t, \beta_1) + y(u+t, \beta_2)}{2}, \qquad (6)$$

where $\tilde{y}(u, \frac{\beta_1+\beta_2}{2})$ denotes the pixel u of the interpolated projection at angle $\frac{\beta_1+\beta_2}{2}$. t denotes the motion of structures that is calculated by

$$t = \text{argmin} \| y(\mathcal{N}_{u-t}, \beta_1) - y(\mathcal{N}_{u+t}, \beta_1) \|_1, \qquad (7)$$

where $\mathcal{N}_{u-t}$ denotes the indices of the neighboring pixels of $u-t$. The feature preserving interpolation looks for the symmetric shift t that has minimum l_1 distance between two local structures. The search range of t is determined by the downsampling rate and system geometry. For an interpolated view that is not equidistant between measured views, the motions of the structures are also assumed to be linear with respect to the angle of the interpolated view as

$$\begin{aligned}\tilde{y}(u, &\alpha\beta_1 + (1-\alpha)\beta_2) = \\ &\alpha \cdot y(u - 2(1-\alpha)t, \beta_1) + (1-\alpha) \cdot y(u + 2\alpha t, \beta_2),\end{aligned} \qquad (8)$$

where $0 < \alpha < 1$ denotes an arbitrary interpolation fraction.

D. Restore high frequency structures

With the interpolated projection of the high frequency structures, the FBP reconstruction using the upsampled projections has fewer view aliasing artifacts from these structures. The reconstructed high frequency structures image can be directly added back to the aliasing free image from step (a) to proved the final reconstruction.

However, the feature preserving interpolation may still ignore some small structures in the extracted high frequency structures in projection space. The errors in the interpolation may appear as streak artifacts in the FBP reconstruction. Note that, since they are caused by even smaller structures, the magnitudes of the artifacts are also smaller than the correctly restored structures. We propose to apply a soft thresholding before adding to the aliasing free reconstruction. The steps (b)-(d) can be repeated for 2-3 iterations to adaptively restore the high frequency structures. Figure 4 shows restored high frequency structures using direct and adaptive approaches. The adaptive approach has much fewer streak artifacts added to the view aliasing free image.

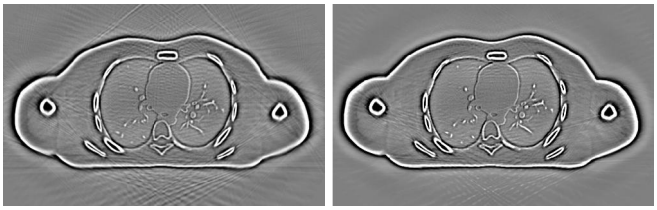

(a) (b)

Fig. 4: FBP restored high frequency structures using direct (a) and adaptive (b) approaches. Display window [-250 250] HU.

III. Simulations

We tested the proposed algorithm using two CT system geometries. The first one is Siemens SOMATOM 32 row clinical CT scanner for a thorax scan, which has 721 views over 232 degrees. The curved detector pixel spacing is 1.407 mm in the latitudinal direction. The second one is Siemens Artis Zeego C-arm CT scanner for a head scan, which has 496 views over 210 degrees. The flat panel detector with 2x2 binning has pixel spacing of 0.3 mm in the lateral direction.

The polychromatic projection data were simulated using modified XCAT numerical phantoms. Poisson noise was added to the simulated data to test the robustness of the proposed algorithm. The views were downsampled by 6 and 8 for the SOMATOM data, and by 4 and 6 for the Zeego data. We compared the proposed algorithm with the linear sinogram interpolation method.

IV. Results

Figure 5 shows reconstruction results of the linear interpolation and the proposed methods. The top two rows used 121 projections (downsampled by 6) of the thorax phantom, and the bottom two rows used 124 projections (downsample by 4) of the head phantom. The proposed method using adaptively merged images has fewer streak artifacts in both test cases. The errors in the azimuthal directions are smaller than are seen in images generated using the linear interpolation method. The proposed methods generated more errors in the radial direction caused by the shifting in the interpolation.

Mean absolute errors of the reconstructions with different downsampling rates are summarized in Table I. The proposed method using the adaptive restored image has smaller mean absolute error, which agrees with visual results in Figure 5. Moreover, higher downsampling rates cause large errors because of the additional missing data and noise. We have tested the proposed method with noisier data; the interpolation is robust to noise. Denoising methods such as bilateral filter may be applied in the reconstruction process.

V. Conclusion

In this work, we described a novel FBP-based algorithm for sparse view CT reconstruction. Numerical simulation showed that the proposed method reduces streak artifacts and azimuthal blurring caused by sparse views. The total reconstruction time of the proposed method is about 2-4 times that of normal FBP reconstruction using full views. This algorithm

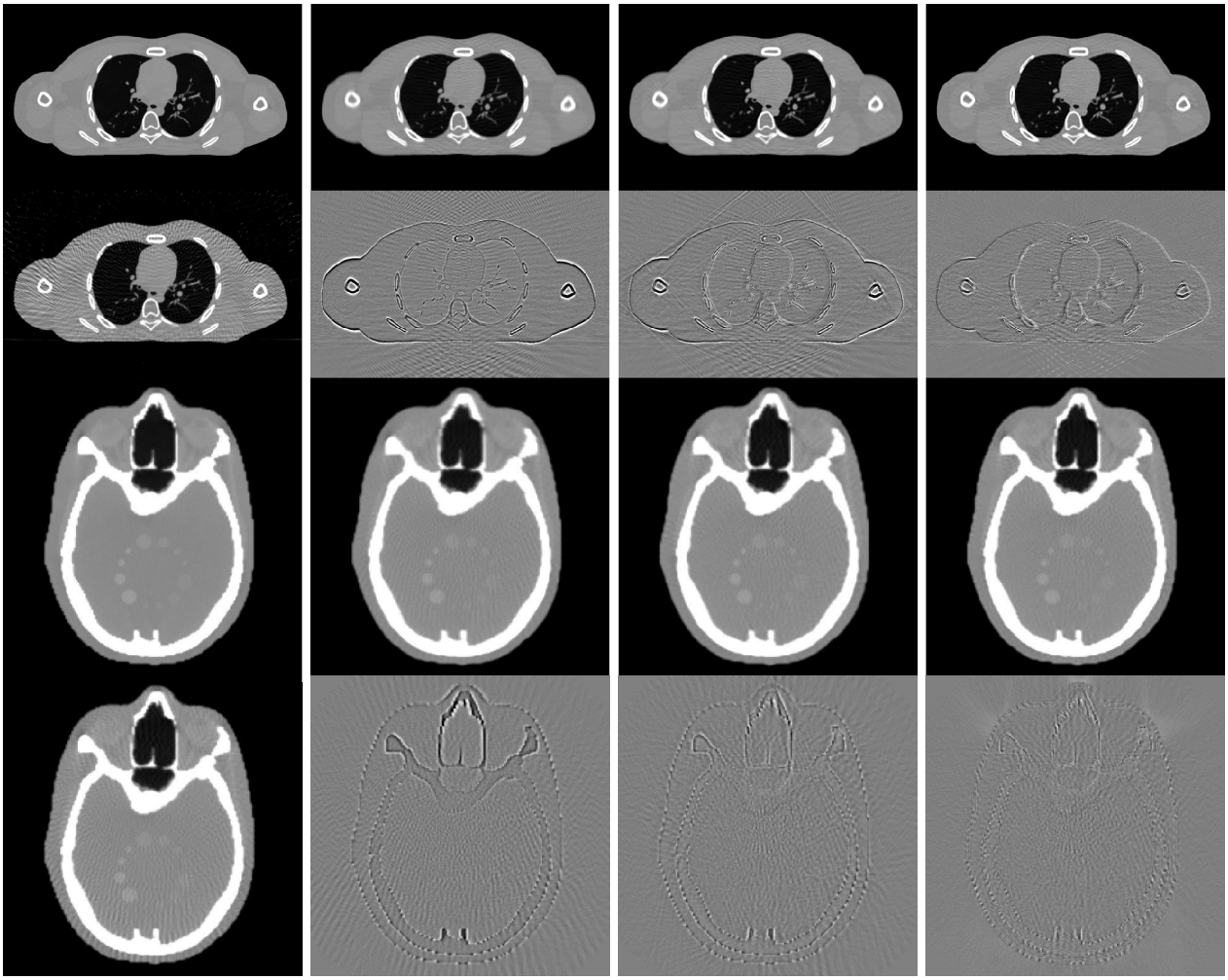

(a) (b) (c) (d)

Fig. 5: Reconstruction results of the liner interpolation and the proposed methods. Column (a) top: FBP reconstruction without view downsampling (ground truth); (a) bottom: FBP reconstruction of downsampled data. Column (b) linear interpolation method and difference with the ground truth. Column (c) proposed method using directly merged image and difference with the ground truth. Column (d) proposed method using adaptive merged image and difference with the ground truth. The display window for reconstruction is [-750 750] HU; and for difference image is [-250 250] HU.

TABLE I: Mean absolute errors (in HU) of the reconstructions with different downsampling rates.

Phantom	Linear interpolation	Direct merge	Adaptive merge
Thorax by 6	26	24	19
Thorax by 8	34	32	23.5
Head by 4	15	13	12
Head by 6	24.5	21	18

may be used when reconstruction time is critical, frame rate is limited and/or dose reduction via reduction in number of views is desired. Comparison with iterative algorithms is the subject of future work.

REFERENCES

[1] J. Tang, B. E. Nett, and G.-H. Chen, "Performance comparison between total variation (TV)-based compressed sensing and statistical iterative reconstruction algorithms.," *Phys. Med. Biol.*, vol. 54, no. 19, pp. 5781–5804, 2009.

[2] J. Bian, J. H. Siewerdsen, X. Han, E. Y. Sidky, J. L. Prince, C. a. Pelizzari, and X. Pan, "Evaluation of sparse-view reconstruction from flat-panel-detector cone-beam CT.," *Phys. Med. Biol.*, vol. 55, pp. 6575–99, Nov. 2010.

[3] X. Pan, E. Y. Sidky, and M. Vannier, "Why do commercial CT scanners still employ traditional, filtered back-projection for image reconstruction?," *Inverse Probl.*, vol. 25, p. 1230009, Jan. 2009.

[4] R. R. Galigekere, K. Wiesent, and D. W. Holdsworth, "Techniques to alleviate the effects of view aliasing artifacts in computed tomography," *Med. Phys.*, vol. 26, no. 6, p. 896, 1999.

[5] H. Zhang and J.-J. Sonke, "Directional sinogram interpolation for sparse angular acquisition in cone-beam computed tomography.," *J. Xray. Sci. Technol.*, vol. 21, pp. 481–96, Jan. 2013.

[6] M. Pohlmann, M. Berger, A. Maier, J. Hornegger,and R. Fahrig "Estimation of missing fan-beam projections using frequency consistency conditions," *Proc. of the third int. conf. on image formation in X-ray CT*, pp. 203-207, 2014.

[7] T. Chen, "Adaptive temporal interpolation using bidirectional motion estimation and compensation," in *Proceedings. Int. Conf. Image Process.*, vol. 2, pp. II–313–II–316, IEEE, 2002.